High Speed Imaging of Inhomogeneous Ignition in a Shock Tube

A.M. Tulgestke, S.E. Johnson, D.F. Davidson, R.K. Hanson
Stanford University
Stanford, CA, USA

1 Introduction

Modern engines employing low-temperature combustion strategies have been plagued by problems of knock and flashback stemming from irregular auto-ignition behaviors at low temperatures [1]. In order to develop an understanding of ignition behavior at low temperatures, several recent studies have been carried out on the combustion behavior of real and surrogate fuels at temperatures below 1000 K. These studies have increased awareness of the existence of inhomogeneous ignition regimes in common zero-dimensional experimental reactors.

Localized point ignitions were observed using sidewall Schlieren and shadowgraph diagnostics during the combustion of several single component fuels in rectangular shock tubes [2,3]. Similarly, localized point ignitions were observed during iso-octane combustion in a rapid compression machine by high-speed imaging through a transparent endwall [4]. These studies have shown that experiments run within inhomogeneous ignition regimes are susceptible to strong influence from point ignitions, leading to inconsistency in measured ignition delay times. In a previous work, the authors observed fluctuation by a factor of 2, of measured heptane ignition delay times at specific temperatures between 800 and 1000 K [5].

Explanations for the cause of inhomogeneous ignition regimes in experimental reactors center around the formation of localized hot-spots within the unburned gas. For shock tubes specifically, discussed sources of hot-spots include shock bifurcation [6,7] and small particulates [8,9]. In this work, point ignitions during the low temperature combustion of several fuels are studied. Ignition events are visualized by high-speed imaging through transparent shock tube endwalls. Single component fuels and real fuel blends are studied. Shock tube parameters of wall heating and diaphragm material are varied.

Correspondence to: amtulges@stanford.edu

2 Experimental Setup

Two Stanford shock tubes were utilized in this study. Experiments were duplicated in the Stanford aerosol shock tube (AST), described in detail by Campbell et al. [10], and the Stanford kinetics shock tube (KST), described in detail by Oehlschlaeger et al. [11]. The driven sections of these shock tubes measured 11.53 cm in diameter by 9.73 m long, and 14.13 cm in diameter by 8.54 m long, for the AST and KST, respectively. Diaphragms were made from 0.010 inch thick Lexan and 0.008 inch thick stainless steel. Lexan diaphragms were ruptured by a crossed-blade fixture placed inside the shock tube adjacent to the diaphragm. Steel diaphragms were scribed along a cross to a depth of 0.005 inches, prior to installation within the shock tube. Test gas components of Ar and O_2 were obtained from Praxair (>99.9%). Normal heptane and iso-octane were obtained from Sigma-Aldrich (99+%).

The primary diagnostic utilized in this study was high-speed visible imaging. A Phantom™ V710 high-speed camera captured visible light reflected from a 2 inch diameter imaging mirror placed along the centerline of the shock tube. The imaging mirror was placed 150 cm away from the 1 inch thick fused quartz shock tube endwall. The camera focus was placed at a plane approximately 10 cm away from the endwall, inside the shock tube. Images were captured at a rate of 10kHz with an exposure time of 99µs. The spectral range of the camera was approximately 350-1050 nm. The camera recorded emission that originated from the reacting gas in the shock tube, as well as backscattered light from a halogen floodlamp placed next to the imaging mirror. Additional diagnostics included: fuel concentration measurement by IR laser absorption at 3.39µm, OH* emission monitoring at 306 nm, and sidewall pressure measurement using a Kistler™ 603B1 transducer. These additional diagnostics were located 2cm from the shock tube endwall. A schematic of the diagnostic setup can be seen in Figure 1.

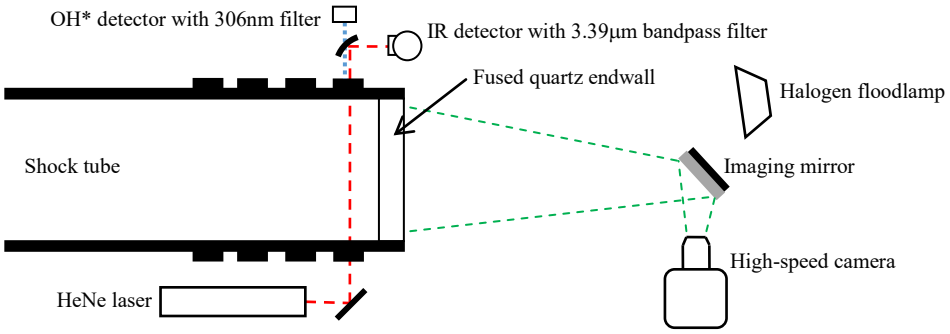

Figure 1. Diagnostic Setup

3 Results

Three fuels were investigated in this study: n-heptane, iso-octane, and Jet A. These fuels were mixed with an oxidizer of 21% O_2 / 79% Ar (airgon) to an equivalence ratio of 0.5 in a magnetically stirred, stainless steel mixing tank. When using Jet A, the mixing tank was heated to 120°C and the shock tube driven section was heated to 80°C. Gas mixtures were injected into the shock tube and subsequently shock heated to 800-1000 K, 1-2 atm. Images detailing the ignition behavior were recorded.

In both shock tubes, when using Lexan or steel diaphragms, several small particles were observed within the test gas. Particles were observed by backscattering of light from the halogen floodlamp, and are thought to originate from the diaphragms. Samples of the particles collected from the end of the shock tube after each shock matched the appearance and texture of the diaphragm that was burst during the experiment. Sampled particle sizes varied from approximately 0.3-3.0 mm for both Lexan and steel

diaphragms. Arrival of the particles near the endwall of the shock tube was observed to occur within 5 ms after reflection of the incident shock wave from the endwall. For a typical shock velocity of 680 m/s, particles originating at the diaphragm would have traversed the length of the shock tube in approximately 18 ms, from the time of rupture of the diaphragm. We conclude that some particles inevitably remained within the shock tube in spite of rigorous cleaning efforts, e.g. by scrubbing the entire length of the shock tube with cotton cloths sprayed with acetone. These free particles were initially distributed throughout the length of the shock tube, and were therefore able to arrive at the endwall sooner than any originating from the diaphragm, in a given shock experiment.

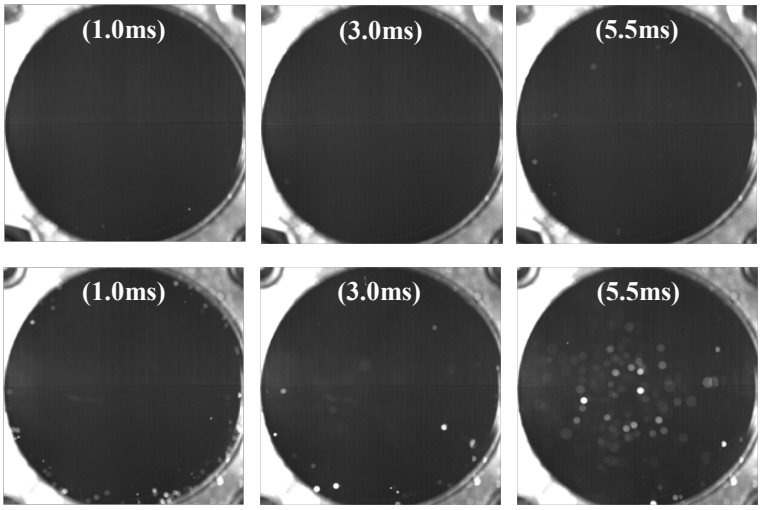

Figure 2. Comparison of number of particles observed during an experiment in the KST.
Top Row: iso-octane/airgon, ϕ=0.5, T=966K, P=1.5atm, Lexan diaphragm;
Bottom Row: n-heptane/airgon, ϕ=0.5, T=1000K, P=1.6atm, Steel diaphragm.

Figure 2 compares the number of particles observed for each diaphragm material during a typical experiment. Distinctly more particles were observed during experiments run with steel diaphragms than were observed when Lexan diaphragms were used. For each of the two experiments shown, the shock tube was cleaned immediately prior, as well as for each of 3 prior experiments. Figure 2 also shows that more particles were present 5.5ms after arrival of the incident shock wave, than were present after 3ms. All experiments with steel diaphragms showed a large number of particles appear nearly simultaneously, 4-5ms after reflection of the incident shock wave, that are thought to originate from the diaphragm that was burst during the experiment.

Flames often formed around the particles within the shock tube. As seen in Figure 3, the observed flames had a bright spot at their core that was due to a reacting particle at the center of the flame. Similar bright cores have been observed in flames imaged in other experimental reactors [4].

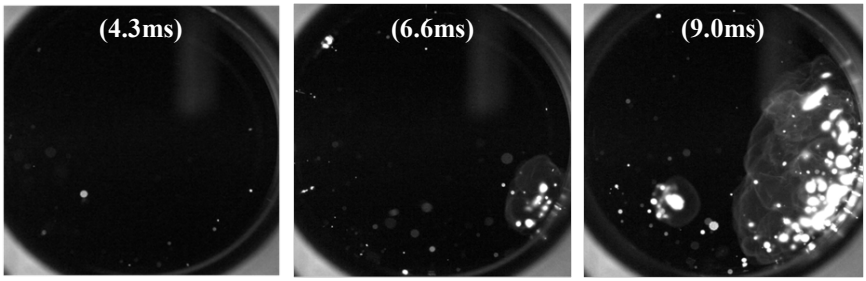

Figure 3. Particle-centered ignition in the AST. n-heptane/airgon, ϕ=0.5, T=970K, P=1.4atm, Lexan diaphragm.

Flames that originated from particles were observed in all experiments. Immediately prior to ignition, these particles would often explode. Typical particle explosions are shown Figures 4 and 5. Particles of both Lexan and steel exhibited similar explosive behavior. Not all particles exploded, nor did all particle explosions lead to flames.

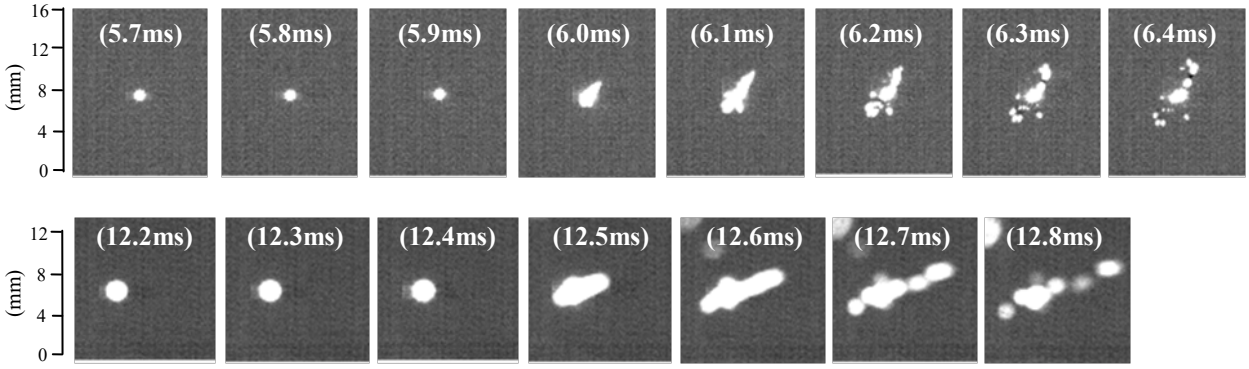

Figure 4. Particle explosions in the KST. Top Row: Jet A/airgon, ϕ=0.5, T=933K, P=1.3atm, Lexan diaphragm; Bottom Row: n-heptane/airgon, ϕ=0.5, T=975K, P=1.6atm, Steel diaphragm.

The subsequent formation of a flame, following a particle explosion, is detailed in Figure 5. It is seen that the flame formed around the exploding particle; in this case within 0.5ms from the start of the explosion. The flame then grew continuously, over a period of several milliseconds, until it consumed all of the fuel within the cross-section of the shock tube.

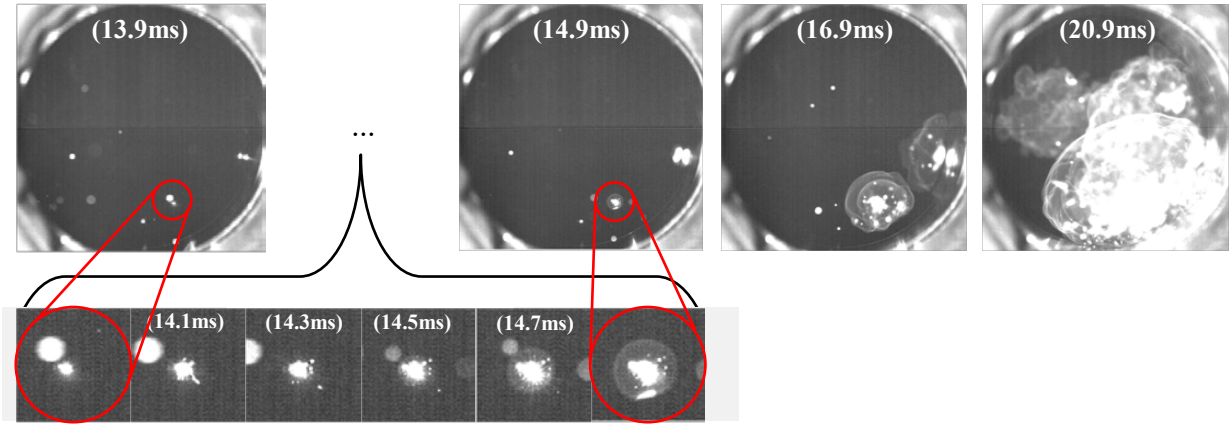

Figure 5. Particle explosion igniting a flame in the KST. Jet A/airgon, ϕ=0.5, T=931K, P=1.3atm, Lexan diaphragm.

The inhomogeneous flames formed after particle explosions influence line-of-sight measurements made from the sidewall of the shock tube. Figures 6 and 7 show the measured HeNe laser absorption and OH* emission during iso-octane oxidation in the AST, and Jet A oxidation in the KST, respectively. The OH* rise and HeNe absorbance (fuel) decay occur more gradually in Figure 6, than the sharper changes in Figure 7. This occurs in spite of similar inhomogeneous flame formation imaged during the two shocks. The difference in signal decay time is thought to be due to the axial locations of the inhomogeneous flames; those farther away from the sidewall diagnostics' location associated with sharper signal changes. The quality of the focus of the flames in the images supports this interpretation. In both experiments, minimal pressure rise occurred during combustion as the majority of the fuel was consumed slowly by the inhomogeneous flames. In such cases, measurements of ignition delay times and species time-histories that can be accurately interpreted with zero-dimensional modeling, cannot be made.

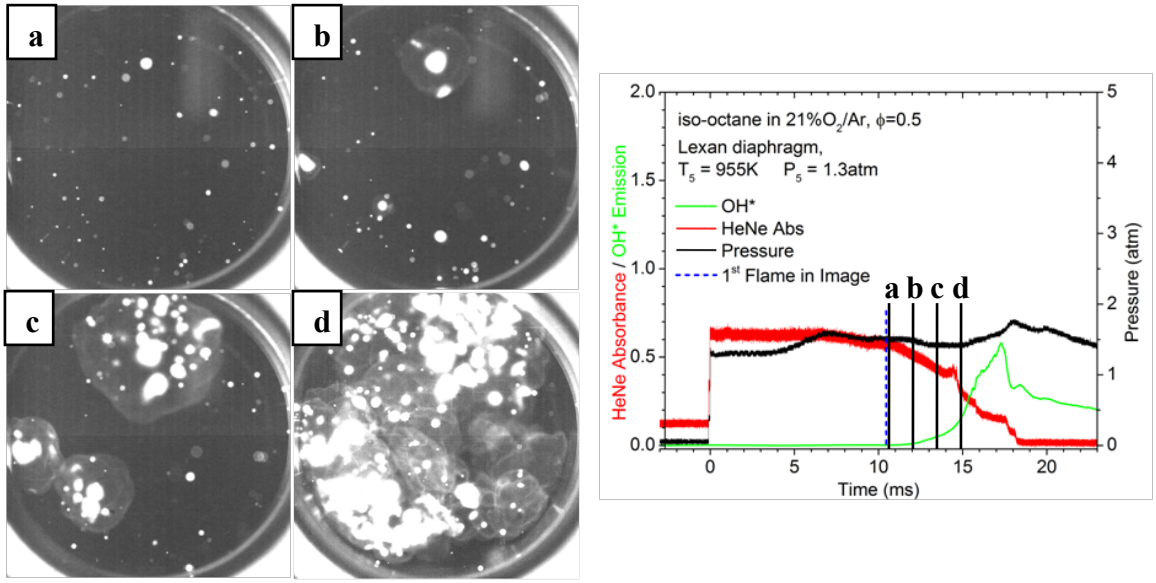

Figure 6. Inhomogeneous flames causing gradual changes in sidewall diagnostic measurements.

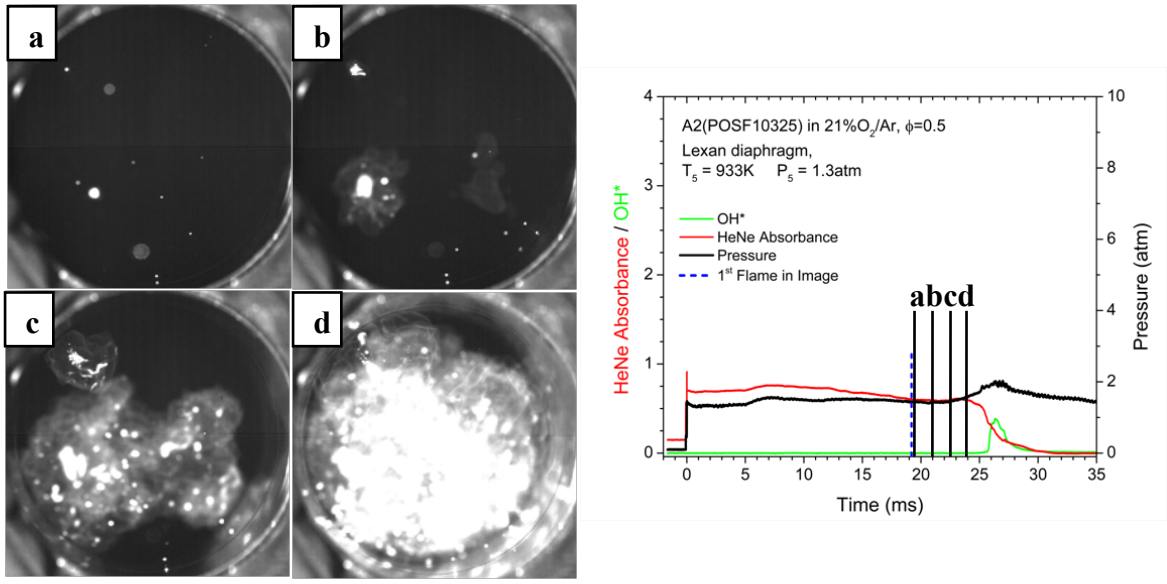

Figure 7. Misleading sidewall diagnostic measurements.

4 Summary

In the present study, inhomogeneous ignitions of real and surrogate fuels were imaged following small particle explosions in two shock tubes. These experiments were carried out at low temperatures (900-1000 K) and low pressure (1-2 atm). Particles within the shock tubes were found to match the material of the diaphragm burst during the experiment. The particles were found to arrive near the endwalls of the shock tubes less than 5ms after reflection of the incident shock wave. Particle explosions were observed for several milliseconds after arrival of the particles, often leading to inhomogeneous

ignition of the fuel. Flames formed from particle explosions were shown to influence the line-of-sight measurements made from the sidewalls of the shock tubes. The diaphragm material used to create shock waves was varied between Lexan and steel. Distinctly more particles were observed during experiments using steel diaphragms than those using Lexan diaphragms. Both diaphragm materials showed explosive behavior leading to flames.

5 Acknowledgements

This work was supported by the U. S. Army Research Laboratory and the U. S. Army Research Office under contract/grant number W911NF1310206.

References

[1] Richards GA, McMillian MM, Gemmen RS, Rogers WA, Cully SR. (2001). Issues for low-emission, fuel-flexible power systems. Progress in Energy and Combustion Science. 27: 2: 141-169.

[2] Heufer KA, Olivier H. (2011). Optical Investigation of Shock Induced Ignition of Different Biofuels. 23rd ICDERS.

[3] Fieweger K, Blumenthal R, Adomeit G. (1997). Self-ignition of S.I. engine model fuels: A shock tube investigation at high pressure. Combustion and Flame. 109: 4: 599-619.

[4] Mansfield AB, Wooldridge MS. (2015). Low-temperature ignition behavior of iso-octane. Fuel. 139: 1: 79-86.

[5] Davidson DF, Tulgestke AM, Strand C, Campbell M, Hanson RK. (2015). Rapid Chemiluminescent Imaging Behind Reflected Shock Waves. ISSW30. *in press*.

[6] Weber YS, Oran WS, Boris JP, Anderson JD. (1995). The numerical simulation of shock bifurcation near the end wall of a shock tube. Phys Fluids. 7: 10: 2475-2488.

[7] Grogan KP, Ihme M. (2015). Weak and strong ignition of hydrogen/oxygen mixtures in shock-tube systems. Proc. Combust. Inst. 35: 2: 2181-2189.

[8] Elsworth JE, Haskell WW, Read IA. (1969). Non-uniform ignition processes in rapid-compression machines. Combustion and Flame. 13: 4: 437-438.

[9] Pfahl U, Fieweger K, Adomeit G. (1996). Self-ignition of diesel-relevant hydrocarbon-air mixtures under engine conditions. Symposium (International) on Combustion. 26: 1: 781-789.

[10] Campbell MF, Tulgestke AM, Davidson DF, Hanson RK. (2014). A second-generation constrained reaction volume shock tube. Review of Scientific Instruments. 85: 5.

[11] Oehlschlaeger MA, Davidson DF, Hanson RK. (2004). High-Temperature Thermal Decomposition of Isobutane and n-Butane Behind Shock Waves. J Phys Chem A. 108: 4247-4253.